Mobility at the TpA Cleavage Site in the T_3A_3-Containing *Aha*III and *Pme*I Restriction Sequences†

Michael A. Kennedy,*,‡,§ Sirkku T. Nuutero,§ Jeffery T. Davis,§ Gary P. Drobny,‡,§ and Brian R. Reid*,§,∥

Battelle Pacific Northwest Laboratories, Richland, Washington 99352, and Departments of Chemistry and Biochemistry, University of Washington, Seattle, Washington 98195

Received February 26, 1993; Revised Manuscript Received May 21, 1993

ABSTRACT: Lefevre et al. originally observed conformational transitions at the TpA step in the TTAA Pribnow box sequence of the trp promoter [Lefevre, J.-F., Lane, A. N., & Jardetzky, O. (1985) *FEBS Lett. 190,* 37–40]. In 500-MHz ^{1}H NMR studies on the T_nA_n-containing DNA oligonucleotides [d(CGAGGTTTAAACCTCG)]$_2$, [d(GCTCCTTTAAAGGAGC)]$_2$, and [d(GCCGTTAACGGC)]$_2$, we observe that, in addition to the H2 proton (which resides in the minor groove of DNA), the H8 proton of the first adenine (which resides in the major groove) is also broadened due to motion at the TpA junction. In analogous 16-mers where the T_3A_3 segment has been replaced by an A_3T_3 sequence, and therefore contains CA, GA, and AT steps (but no TA steps), all adenine proton resonances are narrow, indicating that the broadening occurs only at TpA steps. Assuming chemical exchange in the form of conformational dynamics, e.g., oscillation of the purine base about the glycosidic torsion angle, the experimental 500-MHz ^{1}H $T_{1\rho}$ and 2D-NOESY data were used to constrain the correlation time of the internal motion to a range between the T_1 and $T_{1\rho}$ minima. Calculated line shapes using a two-site exchange model indicate that the motion has an amplitude of 20–50° with an associated τ_c of ca. 1.6×10^{-4} to 1.0×10^{-5} s rad^{-1}, respectively. The mobility appears to be a consequence of the structure at the TpA junction which is characterized by (1) a wide minor groove between two regions of narrow minor groove, (2) an unusual average orientation of the adenine heterocycle probably resulting from a poor base-stacking interaction of the adenine with the preceding thymine, and (3) a sharp discontinuity in the sugar conformation at the TpA step.

DNA molecules containing A_nT_n tracts exhibit unusually retarded migration during polyacrylamide gel electrophoresis (PAGE) [Marini et al., 1977; for reviews see Hagerman (1988, 1990), Olson et al. (1988), and Trifonov and Ulanovsky (1988)]. Early attempts to explain intrinsic DNA curvature included the "wedge" model (Trifonov & Sussman, 1980) and the "junction" model (Selsing, 1979), and later theoretical studies have addressed the importance of the spine of hydration in the minor groove (Chuprina, 1987) and the structural basis for bending (Chuprina & Abagyan, 1988). The anomalous electrophoretic behavior was proposed by Wu and Crothers (1984) to be due to a coherent planar macrocurvature produced by in-phase microbending within each turn of the DNA helix. Diekmann and Wang (1985) corroborated the abnormal electrophoretic behavior of kinetoplast DNA fragments that share the common feature of periodic repeats of short runs of adenine residues (reporting an observable effect when three to six adenines were present in each repeat). In that study, the abnormal electrophoretic behavior was reported to be accentuated at low temperature and by the addition of Mg^{2+}. Subsequently, Koo et al. (1986) investigated the effect of interruptions in the adenine tract on gel mobility and, by inference, on DNA curvature. They concluded that at least four contiguous adenines are required for anomalous gel migration and that the sequence of the flanking region has only a rather small (5–10%) effect on the magnitude of gel retardation. The temperature and salt dependence of gel migration for curved DNA fragments was studied by Diekmann (1987), who reported an observable effect when three or more adenines were present. Stellwagen and Stellwagen (1990) have studied the effect of PAGE pore size and found that the anomalous gel mobility was still observed at larger pore sizes extrapolated to infinite effective size. The effect of purine base substituents on DNA curvature has been investigated by Diekmann et al. (1987). They showed that anomalous gel migration occurred in AARAA tracts only when the intervening R base-pair is dA:dT, dI:dC (I = inosine), or dP:dT (P = purine), but not when it is dG:dC—suggesting that curvature requires purines with no substituents at the C2 position. Although less pronounced, DNA curvature has also been shown by Diekmann and McLaughlin (1988) to be an intrinsic feature of the *Eco*RI restriction site, G↓AATTC (the down arrow indicates the cleavage point in the restriction sequence). However, they have also shown that the modest curvature of GAATTC sequences increases to quite pronounced curvature in DAATTU sequences (where D = 2,6-diaminopurine) even though D does have a C2 amino group in the minor groove. In an interesting and related observation, Hagerman (1986) reported that related DNA sequences containing repeated symmetrical NT_4A_4N tracts migrate normally in PAGE studies, while repeated NA_4T_4N tracts are strongly retarded. Haran and Crothers (1989) further investigated this behavior and found that ligated decamers containing $NT_2A_5N_2$, NT_3A_5N, and T_5A_5 sequences show retarded mobility, while NT_4A_5 ligated decamers have normal gel mobility. Clearly, the mechanism for DNA curvature, while the focal point of a great deal of research interest, is not

† This work was supported by National Institutes of Health Grant GM 32681. M.A.K. was supported by a Northwest College and University Association for Science Fellowship administered by Washington State University under the DOE Grant DE-FG06-89ER-75522 and by an Alexander Hollaender Distinguished Postdoctoral Fellowship sponsored by the DOE Office of Health and Environmental Research and administered by the Oak Ridge Institute for Science and Education. J.T.D. was supported by NIH NRSA Postdoctoral Fellowship Grant F32 GM14340-01.

‡ Battelle Pacific Northwest Laboratories.
§ Department of Chemistry, University of Washington.
∥ Department of Biochemistry, University of Washington.

0006-2960/93/0432-8022$04.00/0

completely understood, and a number of models have since been proposed to rationalize the relationship between repeated 10-phase AT-rich DNA segments and intrinsic macroscopic DNA curvature (Calladine et al., 1988; Ulanovsky & Trifonov, 1987; Koo & Crothers, 1988; Chuprina et al., 1991a).

Since 1987 there have been several solution-state NMR and combined NMR/molecular dynamics studies of the structure of synthetic DNA oligomers containing A_nT_n and T_nA_n tracts (Kintanar et al., 1987; Gupta et al., 1988; Sarma et al., 1988; Katahira et al., 1988, 1990a,b; Celda et al., 1989; Chuprina et al., 1991b; Kim & Reid, 1992). A general structural feature of A_nT_n tracts has emerged from these NMR studies; the minor groove width, which can be probed in solution by measuring the (n)A-H2 to (m + 1)-deoxyribose-H1′ crosspeak in 2D-NOESY spectra, is progressively narrowed from the 5′ to the 3′ end of an A tract. Katahira et al. (1990b) demonstrated that the initial minor groove width at the N-A step of an NNA_3 segment (when N indicates G, C, or T) depends on the identities of NN; for example, the (n)A-H2 to (m + 1)-H1′ distance for the A of the GA step in $[d(GGAAATTTCC)]_2$ is 3.8 Å, whereas the (n)A-H2 to (m + 1)-H1′ distance for the A of the TpA step in $[d(GGTTTAAACC)]_2$ is ≥4.5 Å. Also, the degree of minor groove width compression appears to be enhanced in self-complementary sequences; for example, in $[d(GGAAATTTCC)]_2$ the (n)A-H2 to (m + 1)-H1′ distance is compressed to 3.4 Å at A5 from 3.8 Å at A3, whereas in [d(CGCAAAAAAGCG)]·[d(CGCTTTTTTGCG)] it is only compressed to 3.8 Å at A9 from 4.5 Å at A4. The minor groove width compression that occurs from the 5′ to 3′ direction in adenine runs, as revealed by NMR studies, is most likely related to the mechanism for sequence-dependent formation of UV-induced pyrimidine dimer photoproducts (Brash & Haseltine, 1982). In that study, a 5-fold variation in the frequency of formation of thymine dimers occurred in a TTTTC segment; the propensity for dimer formation was greatest at the 3′ end of the thymine run (i.e., the 5′ end of the complementary adenine run). Thus, it appears that thymine dimer formation is repressed as the minor groove width is narrowed and the cause may be related to a change in the pyrimidine base stacking that is associated with the narrow minor groove structure.

On the basis of adenine H2 line-broadening observations, conformational transitions have been reported to occur at the TpA step in the TTAA Pribnow box of the trp promoter (Lefevre et al., 1985, 1987, 1988; Lane, 1989). Here, we report motional broadening of the H8 as well as the H2 resonances of the adenine base that occurs, in this case, at the TpA cleavage site in T_nA_n-containing DNA oligomers that define the *Aha*III and *Pme*I restriction sequences. From additional NMR observables, limits on the amplitude and rate of the mobility responsible for the line broadening are proposed and the structure at the TpA junction is described. Finally, we discuss the potential implications of this observation on (1) the interpretation of NOESY crosspeaks involving the aromatic protons of the adenine in the TpA junction, (2) the understanding of DNA curvature, and (3) the mechanism for DNA–protein recognition at the binding site of *Aha*III, *Hpa*I, and *Pme*I restriction enzymes.

MATERIALS AND METHODS

Sample Preparation. The DNA oligomers (1) $[d(CGAGGTTTAAACCTCG)]_2$ (28 mg) which contains the *Aha*III restriction sequence, TTT↓AAA, as well as the *Pme*I restriction site, GTTT↓AAAC; (2) $[d(GCTCCTTTAAAGGAGC)]_2$ (28 mg), which contains the *Aha*III restriction sequence, TTT↓AAA; (3) $[d(CGAGGAAATTTCCTCG)]_2$ (20 mg); (4) $[d(CGTCCAAATTTGGACG]_2$ (13 mg); (5) $[d(GCCGTTAACGGC)]_2$ (28 mg), which contains the *Hpa*I restriction site, GTT↓AAC; and (6) $[d(CGCGAA^*TTCGCG)]_2$ (where the asterisk indicates methylation at the exocyclic 6-amino position of A6) (20 mg), which contains the methylated *Eco*RI restriction site, G↓AA^*TTC, were synthesized by the solid-state triester method using cyanoethyl phosphoramidites on an Applied Biosystems 380A DNA synthesizer. The samples were purified on a Sephadex G25 column, and homogeneous fractions, as monitored by gel electrophoresis, were pooled and lyophilized. The samples were dissolved in 0.4 mL of phosphate buffer (pH 7.0) as follows: (1) 400 mM NaCl, 41 mM sodium phosphate, 0.8 mM EDTA; (2) 400 mM NaCl, 41 mM sodium phosphate, 0.8 mM EDTA; (3) 100 mM NaCl, 20 mM sodium phosphate, 0.8 mM EDTA; (4) 400 mM NaCl, 41 mM sodium phosphate, 0.5 mM EDTA; (5) 75 mM NaCl, 30 mM sodium phosphate, 0.7 mM EDTA; (6) 400 mM NaCl, 41 mM sodium phosphate, 0.8 mM EDTA.

NMR Spectroscopy. NMR experiments were performed at 500 MHz either on a Bruker AM-500 spectrometer or on a home-built 500-MHz NMR spectrometer (Gladden and Drobny, unpublished data). One-dimensional spectra were all collected using 8192 complex points with an acquisition time of 0.66 s and a spectral width of 4386 Hz. Each data set was processed using minimal baseline correction and no apodization. The field homogeneity was typically adjusted until the HDO resonance line width was no more than 3–4 Hz. NOESY spectra were collected using the phase-sensitive method (States et al., 1982). In each NOESY spectrum, the mixing time was varied by 10% to eliminate zero-quantum coherence. For NOESY experiments, 2048 complex points in t_2 and 800 points in t_1 were collected with both 2.0- and 10.0-s relaxation delays using a spectral width of 4386 Hz. The NMR data were transferred to an IRIS 4D/20 workstation and processed using the FTNMR program (Hare Research Inc., Bothell, WA). The NOESY data sets were zero-filled to 2048 points in each dimension and apodized with a sine-squared 90° phase-shifted function to 800 points in t_2 and 400 points in t_1. The DQF-COSY experiment (Rance et al., 1983) was performed in the TPPI mode (Drobny et al., 1979; Marion & Wüthrich, 1983) and collected using 2K complex points in the t_2 dimension and 670 points in the t_1 dimension. The data were processed using a 400-point 70° shifted skewed sine bell in t_2 and a 670-point 70° shifted skewed sine bell function zero-filled to 2K complex points in t_1. Nonselective ^1H T_1 measurements were performed using an inversion recovery experiment. T_2 data were collected using a standard Carr–Purcell–Meiboom–Gill spin–echo experiment using composite 180° pulses for inversion and the phase cycling reported by Levitt and Freeman (1981); 30–45 values were used for the variable delay between pulse and echo formation. $T_{1\rho}$ experiments were performed by applying an 18-μs 90° pulse followed by a variable-length spin–lock pulse using a B_1 field strength of ca. 13.8 kHz when on-resonance. The spin–lock time was varied from 1 μs to 1 s using 55 values distributed in a logarithmic fashion. The $T_{1\rho}$ data were collected using a spin–locking field applied at a 1.5-Hz offset. Kopple et al. (1988) have reported that rotating frame relaxation was not affected by up to a 200-Hz offset for even a 2.8-kHz rotating frame field strength, i.e., a 14.3% offset from the carrier. In this case, the experiment was repeated using an on resonance spin–locking field, and no significant change in the decay of

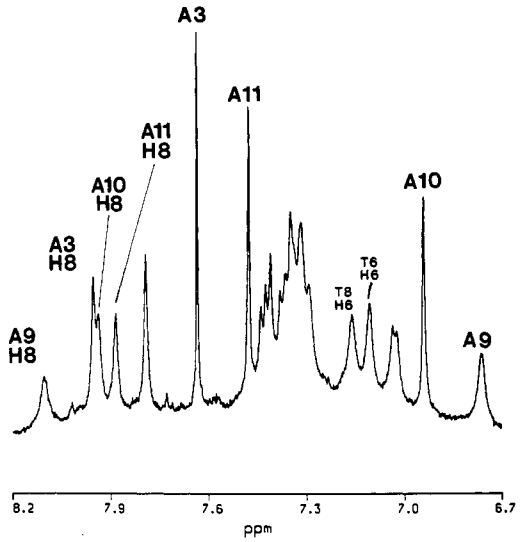

FIGURE 1: 500-MHz ^{1}H spectrum of the aromatic region in [d(CGAGGTTTAAACCTCG)]$_2$ measured at 31 °C. The adenine H2 protons are labeled A3, A9, A10, and A11. The corresponding adenine H8 protons are also labeled.

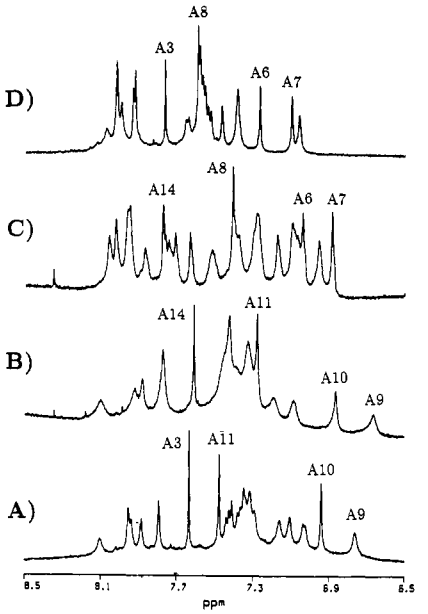

FIGURE 2: 500-MHz ^{1}H specra at 31 °C of the aromatic region of (A) [d(CGAGGTTTAAACCTCG)]$_2$, (B) [d(GCTCCTTTAAAGGAGC)]$_2$, (C) [d(CGTCCAAATTTGGAGC)]$_2$, and (D) d[CGAGGAAATTTCCTCG]$_2$.

the magnetization was observed when compared to data collected using a 21% spin–locking field offset.

RESULTS

Broad Adenine Proton Resonances at T_nA_n Junctions. The aromatic protons of adenine residues at the TpA junctions in T_nA_n sequences (where $n \geq 2$) were observed to be anomalously broadened. As an example, the aromatic proton spectrum of d[(CGAGGTTTAAACCTCG)]$_2$ is shown in Figure 1. The line width of the H2 resonance of A3 (7.65 ppm), which occurs outside the T_3A_3 tract, is 3 Hz and is quite typical for adenine H2 line widths. In marked contrast, the A9-H2 resonance (6.8 ppm) has a line width of 13 Hz and is distinctly broadened by ≈10 Hz. A10-H2 (6.9 ppm), which is one nucleotide downstream from the TpA junction, has a line width of 5 Hz that is intermediate between typical and broadened A-H2 resonances. Furthermore, A11-H2 (7.5 ppm), which is two base-pairs downstream of the TpA junction, has a line width of 3 Hz, i.e., approaching that of a typical adenine. The A9-H2 line width was measured as a function of temperature (data not shown) and was found to behave similarly (maximum line width at 31°) to that of the TpA step adenine in the Pribnow box reported by Lefevre et al. (1988). While the H2 protons reside in the minor groove, the resonance of the A9-H8 proton, which resides in the major groove, has a line width of 14 Hz (see Figure 1), which is about twice as broad as the H8 resonances of A3 (6 Hz), A10 (8 Hz), and A11 (8 Hz).

The dependence of the adenine H2 line width on the identities of N in NAAAN segments was studied by comparing the A9-H2 resonance in [d(GCTCCTTTAAAGGAGC)]$_2$ as well as the various adenine H2 resonances in [d(CGTCCAAATTTGGACG)]$_2$ and [d(CGAGGAAATTTCCTCG)]$_2$ with the corresponding resonances in [d(CGAGGTTTAAACCTCG)]$_2$ (Figure 2). In Figure 2A, the aromatic region of [d(CGAGGTTTAAACCTCG)]$_2$ is reproduced to facilitate visual comparison. In Figure 2B, which shows the aromatic region of [d(CGTCCTTTAAAGGACG)]$_2$, the identical pattern of A-H2 line widths seen in Figure 2A is observed. The A9-H2 at the TpA junction is distinctly broadened, while the next adenine H2, A10-H2, has intermediate line broadening, and by the third adenine in the run, A11-H2, the anomalous line broadening is negligible. However, in Figure 2C, which shows the aromatic region of [d(CGTCCAAATTTGGACG)]$_2$, all adenine H2 resonances have similar and fairly narrow line widths. Note, for example, the similarity in the peak heights/line widths of the A6-H2 and A14-H2 lines in Figure 2C compared with the large difference in the peak heights/line widths of the A3-H2 and A9-H2 lines shown in Figure 2A. In Figure 2D, the four adenine H2 resonances in [d(CGAGGAAATTTCCTCG)]$_2$ again appear narrow and quite similar. This reveals that discrete line broadening occurs neither at the CpA step in C_2A_3 nor at the GpA step in G_2A_3. Furthermore, the effect is not observed at the ApT step in either of the A_3T_3-containing hexadecamers. The anomalous line broadening occurs only at the TpA junction in the T_3A_3 structural unit.

The adenine H2 line widths in T_2A_2- and A_2T_2-containing dodecamers were also compared (Figure 3). The aromatic region of [d(GCCGTTAACGGC)]$_2$ is shown in Figure 3A. The H2 of A7, which occurs at the TpA junction of the T_2A_2 structural unit, is markedly broadened (15 Hz), whereas the H2 of the neighboring A8 is narrow (3 Hz). Furthermore, the A7-H8 (17 Hz) is also about twice as broad as the A8-H8 resonance (10 Hz). In this connection, Lefevre et al. (1988) also reported anomalous line broadening of the TpA adenine H8 proton in a mutant trp operator sequence and has made conflicting statements concerning the TpA adenine H8 line width in the native sequence, reporting excessive line width in one case (Lefevre et al., 1987) but claiming no differential line broadening in another (Lefevre et al., 1988). In Figure 3B, the aromatic region of CGCGA*A**TTCGCG (which contains the *Eco*RI restriction site methylated at the exocyclic 6-amino position of A6 as indicated by the asterisk) is also shown; the methylated sequence was chosen for illustration because of the superior resolution of the adenine H2 resonances—although the adenine H2 resonances of the unmethylated sequence are also both narrow. Neither the A5 nor A6 H2 resonances, nor their H8 resonances, are significantly broadened in AATT or A*A**TT sequences. Clearly, the distinct line broadening occurs only at the TpA junction in the T_2A_2 structural unit, affects the H8 as well as the H2 proton, and does not occur at either adenine position in the A_2T_2 structural unit.

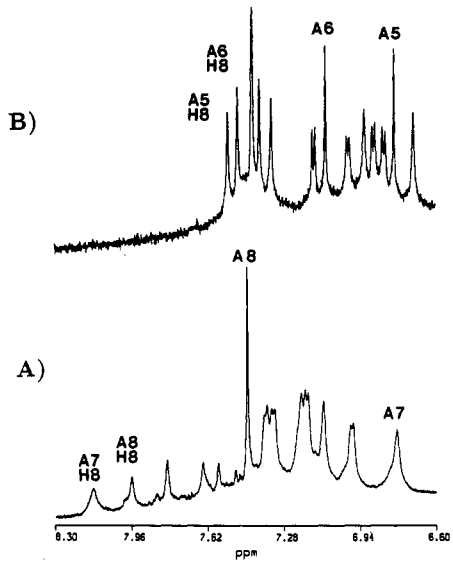

FIGURE 3: 500-MHz aromatic ^{1}H spectra at 31 °C in (A) [d(GCCGTTAACGGC)]$_2$ with the adenine H2 resonances labeled A7 and A8 (the A7-H8 and A8-H8 resonances are labeled—the apparent 2:1 ratio of H2:H8 peak areas reflect ca. 50% exchange of the C8 proton by deuterium after long storage in D_2O) and (B) [d(CGCGA*A**TTCGCG)]$_2$ with the adenine H2 resonances labeled A5 and A6. In each case the corresponding H8 protons are also labeled.

Concerning TpA steps in other contexts, in the sequence TATA, which fits the general sequence, NTAM (where N ≠ T, M ≠ A), we do not observe any unusual broadening of the proton resonances of either adenine in the two TpA steps. We have not yet investigated TpA steps in other possible NTAM contexts, nor have the adenine H2 resonances of TpA steps in sequences that contain T_nAN (where $n \neq 2$ and N = G, C, or T) yet been investigated.

Line-Broadening Mechanisms That Can Be Eliminated. To examine possible contributions other than local motion to the A9-H2 and A9-H8 broadening, we have considered a number of possible line-broadening mechanisms. As can be seen from Figures 1 and 3, different types of aromatic proton resonances in DNA have characteristically different line widths. For example, the broadest aromatic protons are the cytidine and thymidine H6 protons. In addition to dipole–dipole coupling to surrounding sugar protons, the line width of the cytidine H6 includes several hertz of (sometimes unresolved) $^3J_{HH}$ coupling to the vicinal H5 proton. In terms of scalar coupling, all four adenine H2s in Figure 1 should experience the same negligible J coupling since there are no protons or phosphorus atoms within five bonds. Thus, scalar coupling cannot account for the ≈10 Hz of additional broadening observed for the adenine H2 protons. Likewise, the H8 protons of adenine and guanine should experience only a small (1–2 Hz) four-bond scalar coupling with its own sugar H1′ proton. Scalar relaxation of the second kind (Abragam, 1961) could effect the spin–spin relaxation of the adenine H2 through an indirect two-bond interaction if the N1 or N3 nuclei relaxed unusually rapidly. Since the covalent structure of the purine is fixed, the quadrupole coupling constant should not differ from one purine to the next. Therefore, unique quadrupolar relaxation of the N1 and N3 nuclei that differs from that of the the N1 and N3 nuclei of the other adenines in these sequences would occur only if the A9 experienced a unique motion, since modulation of the quadrupole coupling via motion is the dominant mechanism for quadrupolar relaxation. Additionally, to explain the simultaneous broadening of the adenine H8 resonance, the N7 and N9 nitrogen atoms on the five-membered ring of adenine would have to also experience a similar modulation of the quadrupole coupling. The relative mobility of the A9 purine (at the TpA step) will be discussed below.

The extra broadening of thymidine H6 protons is due in part to local fluctuations of the dipolar interaction with the three protons of the rotating methyl group and in part to a small (1–2 Hz) ^4J coupling to the thymine protons. The aromatic protons exhibiting the next broadest line width are the H8 protons of both adenines and guanines. These protons are broadened due to fluctuations of the strong dipole–dipole interactions (Schmidt & Edelheit, 1981) with protons of the sugar ring; for example, in B-DNA the H8 protons of adenine or guanine reside in the major groove and experience dipole–dipole interactions with two close protons, namely their own H2′ (ca. 2.4 Å) and the H2″ of the preceding residue (ca. 2.4 Å). Finally, the adenine H2 protons in the minor groove typically have exceptionally narrow line widths due to the absence of scalar coupling *and* rather weak dipole–dipole interactions because they have no protons in their immediate vicinity in the interior of the minor groove of the DNA duplex (Kearns, 1984).

The fluctuating dipole–dipole interactions that account for the line width of the H8 protons on adenine and guanine bases do not account for the relative line widths of the adenine H2 resonances. Shown in Figure 4A is the 2D-NOESY spectrum of [d(CGAGGTTTAAACCTAG)]$_2$ collected with a 2-s relaxation delay. The NOE intensities from A9-H2 to A9-H1′ (intraresidue) and to A25(A9)-H1′ (interstrand) occur in the same crosspeak due to symmetry. Accordingly, this crosspeak contains two exactly overlapped intensities. However, even if this double crosspeak is treated as a single internuclear interaction, the entire crosspeak corresponds to a distance of ≥4.5 Å. The barely visible (at lower contour) A9-H2 to A10-H1′ crosspeak corresponds to a distance of about 5.0 Å. The A10-H2 shows a stronger cross-strand crosspeak with T24(T8)-H1′ corresponding to ca. 4.3 Å and similar crosspeaks to A10-H1′ and A11-H1′. The most downstream adenine, A11, has a strong cross-strand crosspeak to T23(T7)-H1′ corresponding to ca. 3.9 Å and strong crosspeaks to C12-H1′ and A11-H1′. Finally, A3-H2 has moderate crosspeaks to C31(C15)-H1′, to G4-H1′, and to A3-H1′ that are distinctly stronger than expected in normal B-DNA. Because the adenine H2 resonances typically have longer spin–lattice relaxation times than other protons, a 2D-NOESY was also acquired using a 10-s relaxation delay (Figure 4B); this confirmed that the relative crosspeak intensities are a true measure of relative distances and are not simply due to differences in partial relaxation. The fact that A3, which occurs at a GpA step, has a quite respectable cross-strand crosspeak is not surprising given the observation of Katahira et al. (1990b) that the minor groove width at the GpA step in a GGAAA segment is already rather narrow as reflected in a (n)A-H2 to (m + 1)H1′ distance of 3.8 Å. This implies that the preceding guanine does not totally prevent the formation of a narrow minor groove and appears to be in conflict with the suggestion by Diekmann (1987) and others that a guanine exocyclic 2-amino group prevents the minor groove from narrowing. All of the adenine H8 protons experience at least a few relatively short distances to proximal protons (2.4–3.4 Å) as indicated by several crosspeaks that are strong relative to any adenine H2 crosspeak. This alone accounts for the relative line widths of purine H8 lines compared to adenine H2 resonances. The A11-H2 in [d(CGAGGTTTAAACCTCG)]$_2$ exhibits the strongest set

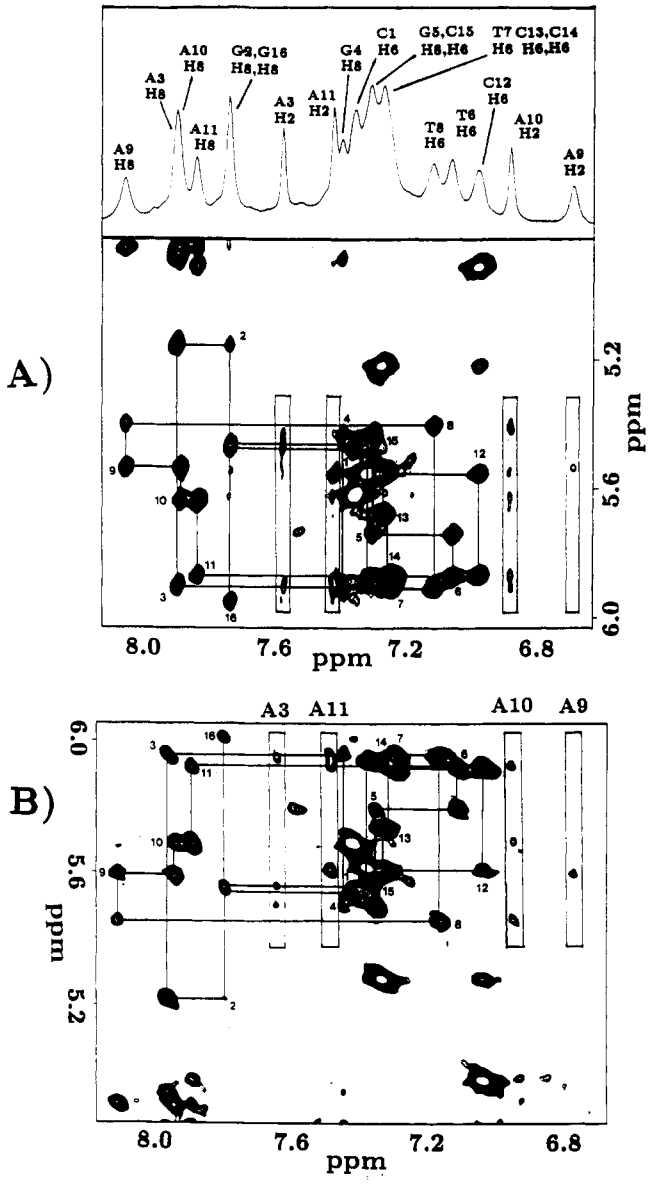

FIGURE 4: 150-ms mixing time 500-MHz ^{1}H NOESY spectrum of [d(CGAGGTTTAAACCTCG]$_2$ in the H8/H6/H2 to H1′ region with (A) 2.0-s relaxation delay and (B) 10.0-s relaxation delay. The projection along the $\omega 2$ axis is shown at the top along with the assignments of each resonance. The boxes indicate regions that contain adenine H2 to (n), (n + 1), and (m + 1) H1′ crosspeaks [where m is the complement of n and (m + 1) is the complement of (n − 1)].

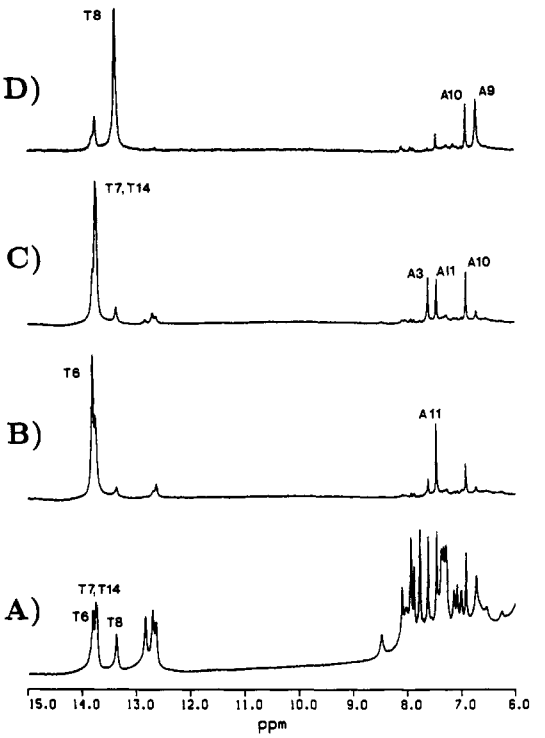

FIGURE 5: (A) 500-MHz ^{1}H NMR spectrum of the imino and aromatic region for [d(CGAGGTTTAAACCTCG)]$_2$ in H_2O at 31 °C. The ^{1}H NOE difference spectra from irradiating (B) the T6-N3H, C) the T7-N3H/T14-N3H, and (D) the T8-N3H imino protons are shown.

of H2 NOESY crosspeaks and, consequently, appears to experience the strongest fluctuations from dipole–dipole coupling. Purely on the basis of the fluctuations of dipole–dipole coupling, A11 would be expected to have the greatest line width of all adenine H2 lines in this sequence. Yet, it is A9-H2, which has the weakest crosspeaks and presumably the weakest or fewest dipole–dipole interactions, that has the broadest line width. The entire columns and rows of NOESY crosspeaks, when investigated over the complete spectral width (data not shown), showed that the strongest crosspeaks involving any adenine H2s are to the H1′ region. Consequently, the relative strength of the summed dipole–dipole fluctuations that affect adenine H2 resonances do not contribute to the anomalously broad line width of A9-H2.

Another potential source of line broadening is DNA site-selective binding of paramagnetic metal ion impurities. The consequence of such binding, in addition to broadening all proximal resonances due to efficient dipolar relaxation with the unpaired electron of the metal ion, is a shortening of the nonselective T_1 of the proximal proton resonances at the ion-binding site (Eisinger et al., 1962). Selective broadening due to site-bound paramagnetic metal ion impurities can be reversed by chelation of the metal ion with EDTA. The nonselective T_1 values of the adenine H2 protons were measured in a solution of [d(CGAGGTTTAAACCTCG)]$_2$ containing 0.8 mM EDTA and were found to be 2.8, 3.5, 3.2, and 2.7 s for the A3-H2, A9-H2, A10-H2, and A11-H2 protons, respectively. Thus, A9-H2 has the *longest* nonselective T_1 of all the adenine H2 protons in this sample and, in fact, has the longest nonselective T_1 of any proton in the entire molecule. The nonselective proton T_1 data, combined with the fact that this sample contained 0.8 mM EDTA, argue strongly against any contribution from paramagnetic impurities to the anomalous line widths of the A9-H2 and A9-H8 resonances.

Accelerated imino proton exchange of the N3H of T24-(T8) could potentially cause a chemical shift dispersion of the complementary A9-H2. This could occur if the isotropic chemical shift of A9-H2 was modulated by solvent exchange or by its hydrogen-bonding status with N1 of A9 through unusually rapid base-pair opening. To examine this possibility, the temperature dependence of the individual imino-exchange rates in H_2O was monitored. The imino proton resonance assignments from NOE difference spectra are shown in Figure 5. Figure 5A shows the imino and aromatic proton region in [d(CGAGGTTTAAACCTCG)]$_2$. In Figure 5B, the imino proton of T6 shows an NOE to the H2 of A27(A11), its complementary partner. In Figure 5C, the T7 and T14 imino protons were irradiated and NOEs observed to the A26(A10) and A29(A3) complements, respectively. Because of the small chemical shift difference among T7, T14, and T6 and the inability to selectively irradiate only T7 and T14, without spillover to T6, a rather strong NOE from T6-N3H to A26-(A11)-H2 is also observed. Finally, in Figure 5D, when the

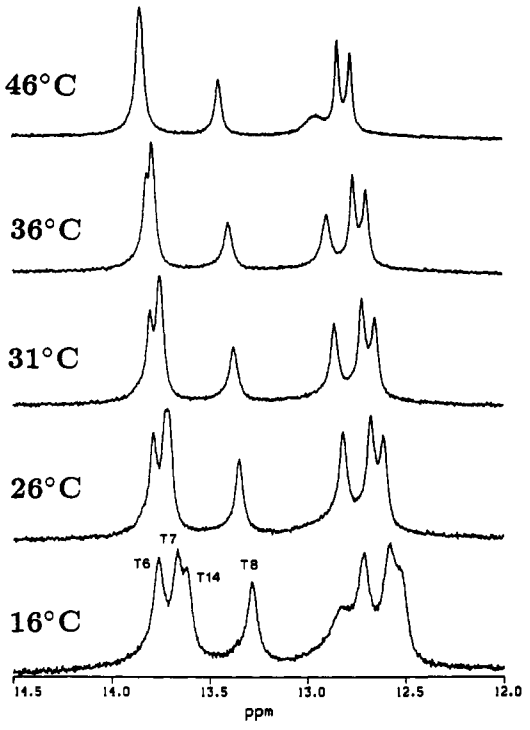

FIGURE 6: 500-MHz ^{1}H spectra of the imino region in [d(CGAGGTTTAAACCTCG)]$_2$ as a function of temperature.

imino proton of T8 is irradiated, NOEs occur to the H2 of A25(A9) and to the H2 of A26(A10).

In Figure 6, the imino proton region of [d(CGAGGTTTAAACCTCG)]$_2$ is shown as a function of temperature ranging from 16 to 46 °C. At 16 and 26 °C, all four thymidine imino protons are observable between 13.3 and 13.8 ppm, each having a similar line width. The guanine imino protons occur between 12.5 and 13.0 ppm. The imino proton of the terminal guanine, G16, is severely broadened due to exchange with water or base-pair opening but is still observable (12.8 ppm) at 16 °C. This demonstrates the line-broadening effect of intermediate to fast chemical exchange. At 26 °C, G16-N1H is fully exchange-broadened and is not observable. At 36 °C, the G2-N1H resonance (initially 12.7 ppm) also begins to exchange-broaden, indicating that exchange/base-pair opening becomes important for the terminal and penultimate base-pairs at 36 °C; at 46 °C it is severely broadened. The line width of the imino proton of T8 (which is paired to the A9 that exhibits the anomalously broadened H2) is essentially unchanged over the temperature range studied and is not distinguishably different from that of the other thymidine imino proton resonances whose complementary adenines exhibit relatively narrow and typical H2 and H8 line widths. This indicates that the A9-H2 resonance is not broadened by abnormal imino proton exchange dynamics at the TpA junction. Consistent with this observation, Leroy et al. (1988) have reported imino-exchange studies on the base-pair opening kinetics for A_nT_n- and T_nA_n-containing segments of DNA. They report that, while imino exchange is inhibited by an apparent unusual stability of the base-pairs within A_nT_n segments, imino exchange at the TpA step in T_nA_n segments is not unusual when compared to random sequence B-DNA. Furthermore, chemical shift dispersion caused by abnormal imino exchange, if it existed, might possibly affect the neraby H2 line width but would probably be negligible at the more distant adenine H8 position and would not explain the experimentally observed line broadening of the A9-H8 resonance.

As judged by 1D NMR spectra, [d(GCTCCTTTAAAGGAGC)]$_2$ initially showed a tendency to form small amounts (≤1%) of hairpin structure presumably forming a T_3A_3 loop, as indicated by thymidine imino resonances appearing at 10.5–11.0 ppm (Hare & Reid, 1986) at salt concentrations below 200 mM. This phenomenon was completely abolished (as can be confirmed by careful inspection of the 10–12 ppm spectrum shown in Figure 5A) by increasing the salt concentration to 400 mM. Hence, in the present study, in addition to preparing NMR samples that were high in DNA strand concentration (ca. 5 mM), all DNA hexadecamer samples were prepared at sufficiently high salt concentrations, e.g., 400 mM, to eliminate the occurrence of imino resonances in the 10–11 ppm range and thus to eliminate the possibility of hairpin loop mobility being the cause of the broad A9-H2 resonance. Furthermore, even if the sample were undergoing a duplex–hairpin equilibrium, the T8 imino proton would have an isotropic chemical shift in the 10.5–11.1 ppm range in the hairpin form (Hare & Reid, 1986) but in the 13.6–13.8 ppm range when base-paired in the duplex form (*vide supra*). Therefore, if the T8 imino proton resonance represented a coalesced line (*vide infra*) due to fast exchange between equal populations of hairpin and duplex forms, an isotropic chemical shift of 12.3 ppm would be expected; this is ≈1 ppm more shielded than the observed chemical shift of 12.3 ppm for the T8-N3H proton. In an attempt to verify the chemical shifts of thymine imino protons in a T_3A_3 hairpin loop, we found that even at a salt concentration of 10 mM phosphate (pH 7.1) with no NaCl and 4 mM strand concentration, the predominant species (≥99%) was the duplex form. Only after further dilution of both the salt and strand concentrations (10× dilution to 0.4 mM DNA in 1 mM phosphate) did the population of hairpin structures become significant; this is in close agreement with the conditions reported for hairpin formation of [d(CGCGTATACGCG)]$_2$ (Wemmer et al., 1985) and [d(CGCGTTTTCGCG)]$_2$ (Hare & Reid, 1986). Moreover, the chemical shift of the H2 proton of an adenine involved in a TATA hairpin loop is deshielded, relative to its base-paired analogue, by up to 0.8 ppm (Wemmer et al., 1985). Note that the hairpin form causes a large **deshielding** of the adenine H2 resonances. However, in the present case, A9-H2 has a chemical shift (6.8 ppm), among the **most shielded** of resonances ever reported for an adenine H2 proton. Furthermore, the A9-H2 resonance is shielded by ≈0.9 ppm relative to the A3-H2 proton resonance (which is narrow), and since A3 occurs outside the T_3A_3 segment and would occur in the stem region of a putative hairpin, it presumably resides in a classical Watson–Crick base-paired segment of DNA in either case. These observations all argue strongly against the presence of any hairpin structures in these samples and militate against base-pair mobility in a hairpin loop being a possible cause of the unusually broadened adenine H2 and H8 resonances.

Effects of Chemical Exchange. The fact that the resonances of adenine H8 and H2 protons, which reside in the major and minor grooves of the duplex, respectively, are both broadened at TpA junctions indicates that the mechanism responsible for the broadening is a function of the entire purine ring. When chemical exchange results from conformational dynamics and the time scale for the dynamics is comparable to the chemical shift dispersion, then changes in line width can occur. The thermodynamics of such proposed conformational transitions has been examined in the trp promoter (Lefevre et al., 1988) and in a mutant of the trp promoter (Lane, 1989). Here we examine the rate and amplitude of the conformational

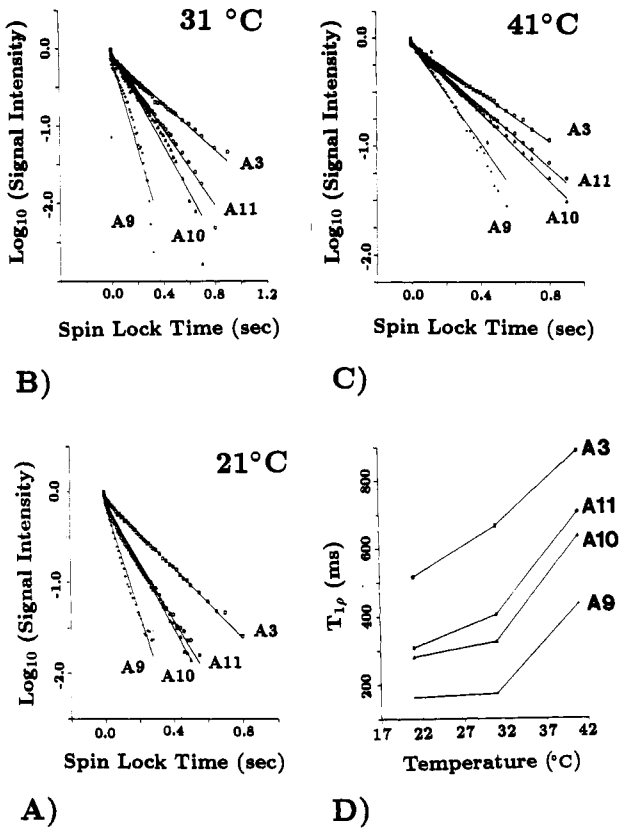

FIGURE 7: Experimental and least-squares fit signal intensity after spin-locking for $[d(CGAGGTTTAAACCTCG)]_2$ plotted as a function of the spin-lock time at temperatures of (A) 21, (B) 31, and (C) 41 °C. The $T_{1\rho}$ values were determined from the least-squares fits to the experimental curves. In (D), $T_{1\rho}$ is plotted as a function of temperature for each residue.

dynamics in the extended T_3A_3 and GT_3A_3C restriction sequences.

Spin–lattice relaxation in the rotating frame (Ailion & Slichter, 1964) is governed in part by $J_1(\omega_1)$ (Strange & Morgan, 1970; Deverell et al., 1970) and is therefore sensitive to motions with rates on the order of the spin-locking field strength, B_1. Rotating frame spin–lattice relaxation has been used by Wang and Ikuta (1989) and Schmitz et al. (1992) to address the question of internal mobility in DNA oligomers. The observed rotating frame spin–lattice relaxation time, $T_{1\rho}$(obs), can be measured by finding the slope of the decay of the signal intensity as a function of the spin-lock time. The measured $T_{1\rho}$ consists of contributions from dipole–dipole interactions and exchange, i.e., $1/T_{1\rho}(\text{obs}) = 1/T_{1\rho}(\text{dd}) + 1/T_{1\rho}(\text{exch})$. Since the A-H2 protons are predominantly isolated from other protons, as shown by the NOESY spectra in Figure 4, in the following discussion it is assumed that $T_{1\rho}(\text{obs}) \approx T_{1\rho}(\text{exch})$ as a first approximation. The $T_{1\rho}$ was measured for the A-H2 protons in $[d(CGAGGTTTAAACCTCG)]_2$, and the experimental data, with least-squares fits of the decay curves, are shown in Figure 7A–C for experiments carried out at 21, 31, and 41 °C, respectively. From Figure 7A–C, the ordering of decreasing $T_{1\rho}$ is A3-H2 > A11-H2 > A10-H2 > A9-H2 at all temperatures. The $T_{1\rho}$ is consistently about 4 times longer than the T_2 values determined from CPMG experiments and from estimates of T_2 based on line-width measurements ($\text{LW} \approx 1/\pi T_2$); for example, for A9-H2 at 31 °C T_2^{CPMG} = 38 ms, T_2^{LW} = 24 ms, and $T_{1\rho}$ = 160 ms. However, when in the fast regime on the $T_{1\rho}$ time scale, all of these values should be about equal, diverging only near the $T_{1\rho}$ minimum. Nevertheless, the A3/A9, A3/A10, etc., ratios of $T_{1\rho}$, T_2^{CPMG}, and T_2^{LW} are consistent for all methods described and the following arguments remain valid (the discrepancy in the absolute values of $T_{1\rho}$, T_2^{CPMG}, T_2^{LW} reflects the uncertainty associated with their measurement; the LW and CPMG values especially suffer from field inhomogeneity and pulse imperfection). The order of decreasing $T_{1\rho}$ can be dictated either by the relative correlation time or by the dipolar coupling strength. If the latter were the major determinant of $T_{1\rho}$, then A9-H2, with the shortest $T_{1\rho}$, should exhibit more NOEs and stronger NOEs than the other adenine H2 protons. This, however, is totally contrary to the NOESY data, where A9-H2 has the fewest and weakest crosspeaks. Since dipolar coupling is completely incapable of explaining the short $T_{1\rho}$ of A9-H2, an altered correlation time is the only remaining parameter that could explain the long T_1/short $T_{1\rho}$/weak NOE/broad line behavior. Therefore, the short $T_{1\rho}$ of A9-H2 reflects an increased correlation time. If the correlation time is the driving parameter, then the residues ordered by decreasing $T_{1\rho}$ values should be the same as the order of increasing T_1 values; this is exactly what is observed experimentally (*vide supra*). In Figure 7D, the $T_{1\rho}$ value is plotted as a function of temperature from 21 to 41 °C and increases for all adenine H2 resonances as the temperature is raised. Assuming that the rate of the purine motion increases with increasing temperature, then the correlation time for all adenines is at, or on the fast side of, the $T_{1\rho}$ minimum.

From the combination of NOESY and $T_{1\rho}$ experiments, the correlation time for the internal motion of the adenine bases must be somewhere between the T_1 minimum and the $T_{1\rho}$ minimum, i.e., from 3.2×10^{-10} to 1.1×10^{-5} s rad^{-1}. To determine if motion on such a time scale could theoretically account for the observed effect on the line width, the expected line shapes for a two-site exchange model were calculated. The line shape resulting from a two-site exchange process assuming equal populations is given by

$$g(\nu) = 2\tau_A(\nu_A - \nu_X)^2/([\nu - {}^1/_2(\nu_A + \nu_X)]^2 + \pi^2\tau^2{}_A(\nu - \nu_A)^2(\nu - \nu_X)^2)$$

where τ_A is the correlation time for the jump and ν_A and ν_X are the isotropic frequencies of the A and X resonances, respectively (Sandström, 1982; Harris, 1983). Both the frequency difference between the two conformers and the rate of interconversion are required to calculate the simulated line shape.

The correlation time at coalescence for two equally populated conformers is given by $\tau_c = 2^{1/2}/\pi(\nu_A - \nu_X)$. Figure 8 shows the correlation time at coalescence as a function of the peak separation in hertz over a 2 ppm span in chemical shift at 500 MHz. As the peak separation approaches zero, the correlation time required for coalescence climbs sharply toward infinity. This, in combination with the $T_{1\rho}$ data, can be used to impose a limit on the low end of the amplitude of the motion leading to coalescence broadening. This is not to say that small-amplitude motions do not occur. In fact, small-amplitude librations of ca. 10° are predicted from solid-state ^{2}H NMR experiments (Kintanar et al., 1989; Alam & Drobny, 1990; Wang et al., 1992b), from EPR experiments (Robinson et al., 1980), and from FPA studies (Allison & Schurr, 1979) but with correlation times that are much too short (ns rad^{-1} to ps rad^{-1}) to cause coalescence broadening for the adenine H2 NMR resonance. The motional amplitude that would correspond to the frequency separation between peaks was estimated from previous studies that have attempted to quantify the magnitude of ring current shifts for the purines

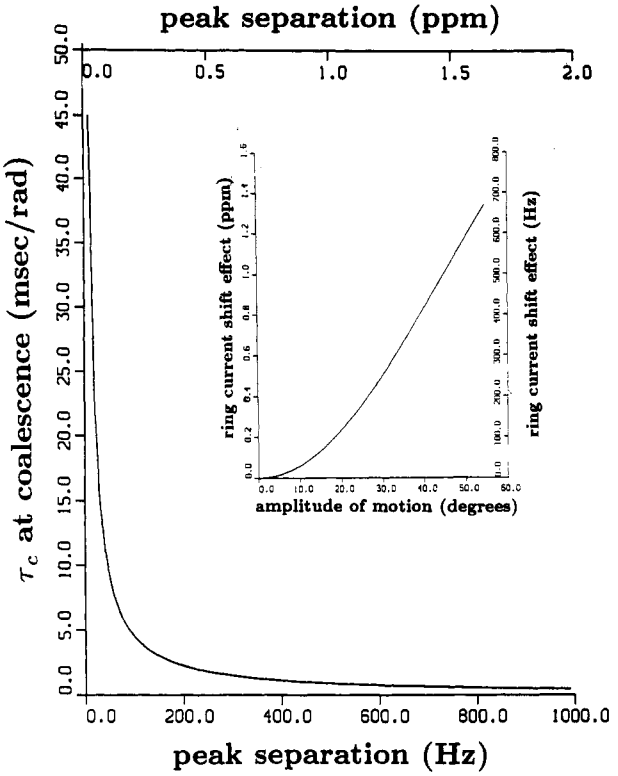

FIGURE 8: Correlation time at coalescence plotted as a function of the peak separation in both frequency and parts per million. (Inset) The ring-current shift effect is plotted in both frequency and parts per million as a function of the amplitude of the motion.

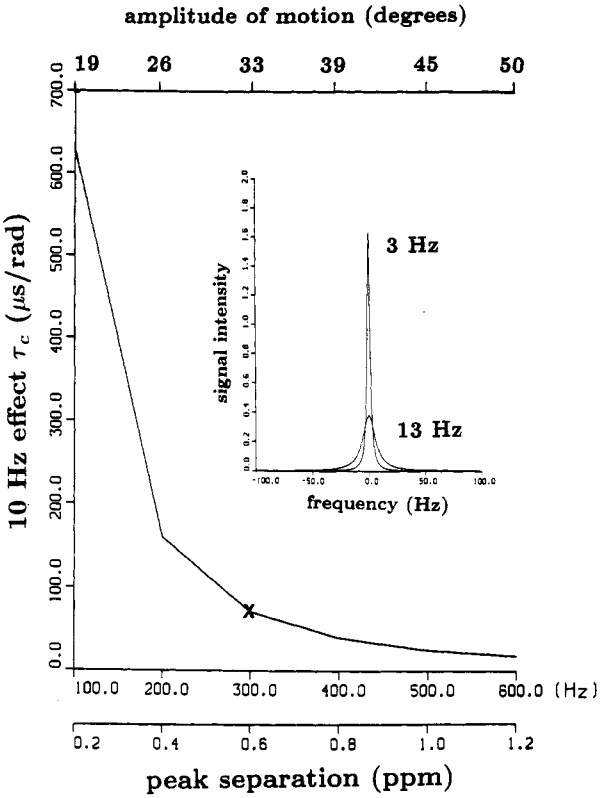

FIGURE 9: Correlation time required to cause 10 Hz of coalescence broadening plotted as a function of the peak separation and the amplitude of the motion. (Inset) The 13-Hz line width resonance that would occur at the X in the curve in Figure 9 that results from a two-site exchange is superimposed on the 3-Hz resonance to show the effect of a 10-Hz coalescence.

and pyrimidines found in nucleic acids (Giessner-Pretrre & Pullman, 1970; Shulman et al., 1973; Kroon et al., 1974; Giessner-Prettre et al., 1976). From these studies, the shielding effect of the ring current for a proton located directly beneath an adenine base [which is the approximate orientation of A7-H2 relative to A8 purine in both $[d(GCGTTTAAACGC)]_2$ (Kim and Reid, unpublished results) and $[d(GCCGTTAACGGC)]_2$ (Kim & Reid, 1992)] at a distance of 3.4 Å should be about 1.33 ppm. At the "magic angle" (54.7°), the ring current shift falls to zero (Waugh & Fessenden, 1957; Johnson et al., 1958). Therefore, if the major determinant of the chemical shift difference between conformers is assumed to be due to changes in ring current shift effects, then, as a first approximation, the chemical shift extrema will occur when (a) the normal from the center of the adjacent adenine heterocycle intersects the H2 proton and (b) the vector to the adjacent H2 subtends an angle of 54.7° (magic angle) to the normal. In the solution-state structure of $[d(GCGTTTAAACGC)]_2$ (Kim and Reid, unpublished results) and of $[d(GCCGTTAACGGC)]_2$ (Kim & Reid, 1992), the heterocycle of the adenine ring is tilted by ≈–20° from perpendicular to the helix axis due to a negative cup at the TpA step. Accordingly, any motion of the adenine base will be about an average conformation which occurs near the center of the P_2 $\cos(\theta)$ angular dependence of the ring current shift effect. Therefore, motion about the glycosidic bond should span the sharpest slope between the extrema of the ring current shift effect. The ring current shift, which obeys a $1/r^3$ P_2 $\cos(\theta)$ dependence (Waugh & Fessenden, 1957; Johnson & Bovey, 1958), is plotted in the inset of Figure 8 as a function of the amplitude of the motion. The maximum chemical shift difference due to changes in ring current effects would be about 1.33 ppm for an oscillation of 54.7°. From Figure 8, the peak separation must be at least 100 Hz because, if the separation were smaller, the magnitude of τ_c would violate the maximum set by the $T_{1\rho}$ observation; from the inset of Figure 8, this limits the amplitude to no less than 19°. While there is no experimental evidence that coalescence in a technical sense has been reached even at 0 °C, motions with rates much faster than the τ_c at the technical coalescence point can cause 10 Hz of coalescence-type broadening, and this is the magnitude observed experimentally. Figure 9 shows a plot of the "10-Hz effect" τ_c vs the peak separation and amplitude of motion. For motions that vary in full amplitude from 19° to 50°, the 10-Hz effect τ_c varies from 630 to 18 μs rad^{-1}. This translates into motions with rates from 2 to 55 kHz. As an example, the inset in Figure 9 shows calculated line shapes for the case indicated by the X in Figure 9, i.e., 10 Hz of coalescence broadening for a motion with an amplitude of 33° and a correlation time of 70 μs rad^{-1}. This simulation effectively reproduces the relative line widths of the adenine H2 resonances observed experimentally.

The range of correlation times producing 10 Hz of coalescence broadening is up to 50 times longer than the $T_{1\rho}$ minimum of 12 μs rad^{-1}. This discrepancy likely originates from two sources. First, the B_1 field strength was estimated using the relationship $\pi/\eta = \tau_\pi\omega_1$, and the $\pi/2$ pulse width was determined by searching for the null spectrum which occurs at $2\tau/\pi_{/2}$. Error in the measurement of $\tau_{\pi/2}$ could lead to an incorrect estimation of the B_1 field strength. Also, the B_1 field strength measured according to this method is most accurate when applied on resonance. In these experiments, the spin–locking field was applied at a 1.5-kHz (3 ppm) offset which, depending on the excitation profile for the pulse, could cause the on-resonance value of 13.8 kHz to be slightly larger than the B_1 field at the aromatic resonance frequencies. An effectively weaker B_1 field would shift the

$T_{1\rho}$ minimum to longer correlation times, thereby improving the agreement between the τ_c limit imposed from the $T_{1\rho}$ data and the τ_c required to reproduce the observed line broadening in line-shape simulations. Note that the locking field offset should not interfere with the measurement of the relative $T_{1\rho}$ values of the A-H2 protons, which are clustered within 1 ppm or 500 Hz of each other, and should experience the same effective flip angle (Bax & Davis, 1985). Second, the magnitude of the ring current shift, which as a first approximation was estimated by including only a single adenine base stacked over the broadened H2 proton, is probably underestimated. The true magnitude of the ring current shift is uncertain, as is the precise position of H2 in the ring-current field. Furthermore, Griessner-Prettre et al. (1976) have demonstrated that the additional ring current shift from a second adenine two base-pairs distanct can be as large as 0.2–0.3 ppm. In the case of the T_3A_3 segments, the mobile adenine is stacked below two adenine bases. If the normalization of the ring current shift effect shown in the inset of Figure 8 is underestimated by 0.2 ppm, then for the same peak separation in Figure 9 a 33° full-amplitude motion would decrease to 26°, or for the same 33° amplitude motion, the 10-Hz effect τ_c would be reduced from 70 to 40 μs rad^{-1}, again improving the agreement with the $T_{1\rho}$-imposed limit on τ_c. Therefore, the amplitude and rate of the motion required to produce the proposed coalescence broadening seem to be consistent with the constraints imposed from the $T_{1\rho}$ data if the uncertainties in the B_1 field strength and the magnitude of the ring current shift are considered. Including the next-nearest-neighbor ring-current effect, the range in τ_c varies from 160 to 10 μs rad^{-1}, which translates into motions with rates varying from 6.2 to 100 kHz and/or total amplitudes in the range of 50° to 20°, respectively.

While A9-H2 lies in a strong shielding gradient due to the cross-strand, $m + 1$ adenine, as deduced from the DNA structure reported by Kim and Reid (1992), A9-H8 appears to lie in a weaker shielding gradient on the basis of the base-stacking diagrams. The A9-H8 proton does, however, experience a sufficient ring-current field to shift its resonance position away from the other adenine H8 resonances. It is possible that the excursion of the A9-H8 proton, due to base mobility, in the weaker shielding gradient is not sufficient to completely explain the 8-Hz broadening of A9-H8 relative to A10-H8. Considering a 2′-endo sugar conformation with $P = 162$, when the adenine base undergoes a ±30° oscillation about the glycosidic bond, at certain orientations the H8-H2′ and H8-H2″ distances shorten by 0.2 and 0.5 Å, respectively. Therefore, the increased magnitude of the dipolar fluctuations may contribute to the broadening of the A9-H8 resonance.

When the aromatic resonances of the adenine base at the TpA junction are broadened due to chemical exchange, i.e., mobility, one might expect the resonances of the bases stacked immediately above or below it to be indirectly broadened by the same mechanism. Specifically, whereas the adenine, because of its own motion, experiences a modulated ring-current shielding effect from the immobile bases stacked above and below, the protons of these adjacent bases should experience similar chemical exchange broadening due to the change in the ring-current effects of the mobile adenine (perhaps to a lesser extent depending on their position in the induced ring current field). In Figure 1, A10-H2 (5 Hz) is broadened more than A11-H2 (3 Hz) and A3-H2 (3 Hz) but less than A9-H2 (13 Hz). In all T_3A_3 sequences we have studied, the broadening of the second adenine H2 is always intermediate between the first (mobile) and the last adenine H2. Similarly, the H8 of A10 (8 Hz), although partially overlapped with A3-H8, is broader than A3-H8 (6 Hz) and about the same width as A11-H8 (8 Hz). Furthermore, on the other side of the TpA junction, the H6 of T8 (12 Hz) is detectably broader than the H6 of the more removed T6 (9 Hz). All of these observations are consistent with a relatively slow (ms rad^{-1} to μs rad^{-1}) mobility of the adenine at the TpA junction and diminished or no mobility further away from the TpA junction.

In a recent study, Schmitz et al. (1992) reported a similar line-width anomaly in the nonsymmetric DNA octamer [d(GTATAATG)]·(CATTATAC)] for A-H2 at the T4-A5 and T12-A13 TpA steps. On the basis of line-width measurements at 300- and 600-MHz ^{1}H frequency, variable-temperature studies, and $T_{1\rho}$ measurements, they were unable to determine the exchange dynamics with any certainty; for example, their field-dependent studies suggested that the exchange was fast on the NMR chemical shift or $T_{1\rho}$ time scale, in contrast to the temperature-dependent line-width measurements which indicated that the exchange occurred in the slow regime. The $T_{1\rho}$ data revealed an exchange lifetime of 0.1 ms for the broadened A5-H2. To explain the data in a self-consistent manner, unequal and temperature-dependent populations of exchanging conformers were required. In contrast, while unequal conformer populations and other more complicated models could certainly be considered, they are not required to account for the observed broadening of the H2 and H8 resonances of adenine at the TpA junctions examined in this study.

Structure at the TpA Junction. In T_nA_n tracts the minor groove is narrow at TpT and ApA steps but abruptly widens at the TpA step, as observed in this work and in comparative studies (Chuprina et al., 1991b) and in quantitative structural studies (Kim & Reid, 1992) on related sequences. The experimentally observed regions of narrow minor groove at the ends of T_nA_n segments are contrary to the conclusions of Burkhoff and Tullius (1988), who suggested that T_nA_n segments should have a uniformly wide minor groove width typical of normal B-DNA; this interpretation was based on the observation that hydroxyl radical-induced cleavage of the phosphodiester linkage was not inhibited in such sequences, while being detectably inhibited in sequences that contain A_nT_n segments. It is clear from the NMR data that the minor groove narrows in the 5′ to 3′ direction in any adenine tract, including T_nA_n tracts, with the initial groove width being only modulated by the upstream flanking context sequence; however, it is also clear that TpA steps cause the narrowed B′ minor groove to locally widen to a normal B-DNA width. In A_4T_4, for example, the patch of B′ structure is established over eight base-pairs while being pulled toward a more typical B-DNA minor groove topology only at the 5′ and 3′ ends and not at the center. In T_4A_4 blocks, however, B′-DNA structure, which is characterized by a narrow minor groove, occurs over only the one or two peripheral base-pairs before being interrupted at the center by the TpA step. This suggests that the minor groove width in T_nA_n segments is far from uniform but actually undergoes large variations, i.e., from narrow to wide to narrow. In fact, if the T_nA_n segment were lengthened, e.g., by increasing n to ≥ 10 (which should allow narrowing of the minor groove to the same extent as in A_4T_4), then inhibition of hydroxyl radical cleavage may well be observed. In terms of DNA curvature, our NMR data imply that simply narrowing the minor groove is not in itself sufficient to produce overall DNA curvature; i.e., the minor groove is progressively compressed from the 5′-adenine to the 3′-adenine in T_3A_3,

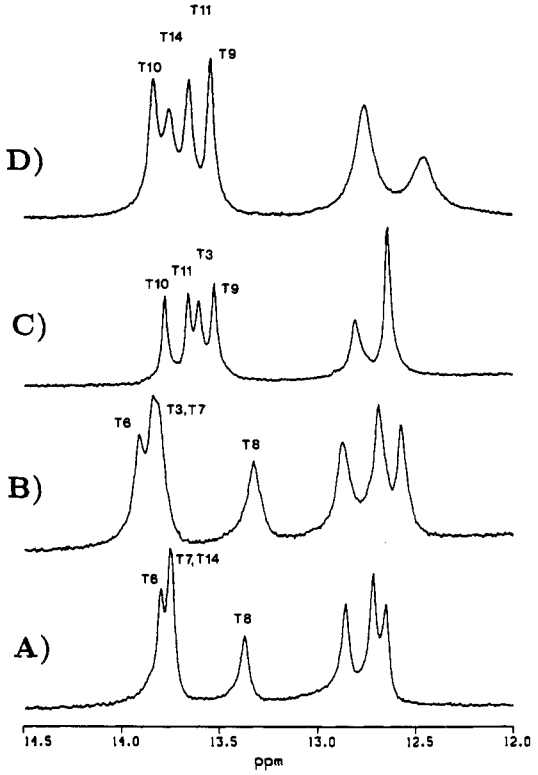

FIGURE 10: 500-MHz ^{1}H spectra of the imino region of (A) [d(CGAGGTTTAAACCTCG)]$_2$ at 31 °C, (B) [d(GCTCCTTTAAAGGAGC)]$_2$ at 31 °C, (C) [d(CGTCCAAATTTGGAGC)]$_2$ at 31 °C, and (D) [d(CGAGGAAATTTCCTCG]$_2$ at 33 °C.

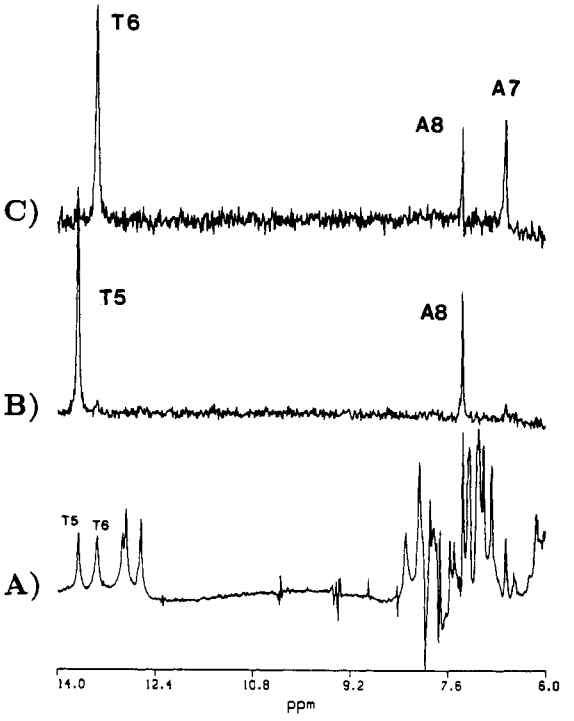

FIGURE 11: 500-MHz ^{1}H NMR spectrum of (A) [d(GCCGTTAACGGC)]$_2$ at 31 °C in H_2O. The NOE difference spectrum from irradiating (B) the T5-N3H and (C) the T6-N3H imino protons are shown.

T_4A_4, A_3T_3, and A_4T_4 sequences, but only the $(N_2A_3T_3N_2)_n$ and the $(NA_4T_4N)_n$ sequences are strongly retarded in PAGE studies (Hagerman, 1986). Since the NT_4A_4N and $N_2T_3A_3N_2$ segments both have twofold symmetry, it would appear that the central TpA kink may either completely or partially cancel the local bending in T_nA_n segments depending not only on their length but also on the nature and length of the intervening 10–2n segments.

In these T_nA_n sequences, the protons at the TpA junction resonate with unusually extreme chemical shifts. For example, the imino proton of the last (3′) thymine of a T_3A_3 tract, i.e., the thymine that is both base-paired to, and immediately upstream of, the putatively mobile A9, is distinctly shielded compared to the other imino protons in T_3A_3 and compared to all of the thymine imino protons in A_3T_3 sequences. Figure 10 shows the imino proton region for two T_3A_3-containing and two A_3T_3-containing hexadecamer duplexes. In both T_3A_3-containing sequences (Figure 10A,B), the chemical shift of the TpA imino proton (13.3 ppm) is shielded by about 0.5 ppm relative to the other thymine imino protons. However, in the A_3T_3 sequences (Figure 10C,D), all of the thymine imino protons are clustered together at 13.6–13.9 ppm. While the line-broadening reflects a dynamic process, the unusual chemical shift of the TpA imino proton indicates an unusual average base conformation at the TpA junction. To determine if this effect is common to all TpA junctions in T_nA_n sequences, the imino spectrum of [d(GCCGTTAACGGC)]$_2$ was examined. Figure 11 shows the imino assignments for [d(GCCGTTAACGGC)]$_2$. (While this sample contained the weakest salt concentration of all samples studied, i.e., 75 mM, there is absolutely no detectable imino resonance in the 10.5–12.0 ppm region which would have indicated an interruption in the normal base-pairing scheme.) Indeed, even in T_2A_2-containing DNA dodecamers (Figure 11A–C), a similar upfield shift is observed for the T6-N3H (13.3 ppm) which is hydrogen bonded to the N1 of A7 that has the broadened H2 in the T_2A_2 unit. The characteristic upfield chemical shift of the thymidine imino protons at the TpA junction in T_nA_n structural units is almost certainly due to a ring-current shift effect related to unusual base stacking at the TpA junction.

Evidence for such unusual base stacking at the TpA junction can be gathered from an analysis of 2D-NOESY stack plots in the base to deoxyribose H1′ region. In an ideal B-DNA duplex with the sequence [d(GCGTTTAAACGC)]$_2$, the (n)H6/H8 to (n – 1)H1′ distance should be in the range 3.50–3.60 Å and the (n)H6/H8 to (n)H1′ distances should be in the range 3.67–3.85 Å. This would manifest itself in linear regime NOESY spectra by a (n)H6/H8 to (n – 1)H1′ crosspeak that has a significantly greater intensity than the corresponding (n)H6/H8 to (n)H1′ crosspeak. Figure 12B shows the expected NOESY spectrum produced by back calculating a classical B-DNA structure; indeed, the A9-H8 to T8-H1′ crosspeak (no. 2 in Figure 12B) is larger than the A9-H8 to A9-H1′ crosspeak (no. 1 in Figure 12B). However, in Figure 12A, which shows the actual experimental NOESY spectrum of this region, this pattern is reversed and the A9-H8 to A9-H1′ crosspeak (3.8 Å) (no. 1 in Figure 12A) is actually larger than the A9-H8 to T8-H1′ crosspeak (4.0 Å) (no. 2 in Figure 12A); the former distance is in the normal range, but the latter distance is much lonter than expected for (n)H8 to (n – 1)H1′ distances in normal B-DNA and is consistent with the observation of large negative cup reported at the TpA junction in [d(CGCTTTAAAGCG)]$_2$ (Kim and Reid, unpublished results) and in [d(GCCGTTAACGGC)]$_2$ (Kim & Reid, 1992). Note that all other (n)H8/H6 to (n)H1′ and (n)H8/H6 to (n – 1)H1′ crosspeak intensities follow the conventional B-DNA pattern; i.e., the (n – 1)H1′ crosspeak is larger than the (n)H1′ crosspeak. The unique orientation of the A9 purine is most likely responsible for the unusual chemical shift of the T6-imino proton in these sequences. A similar explanation is almost certainly responsible for the

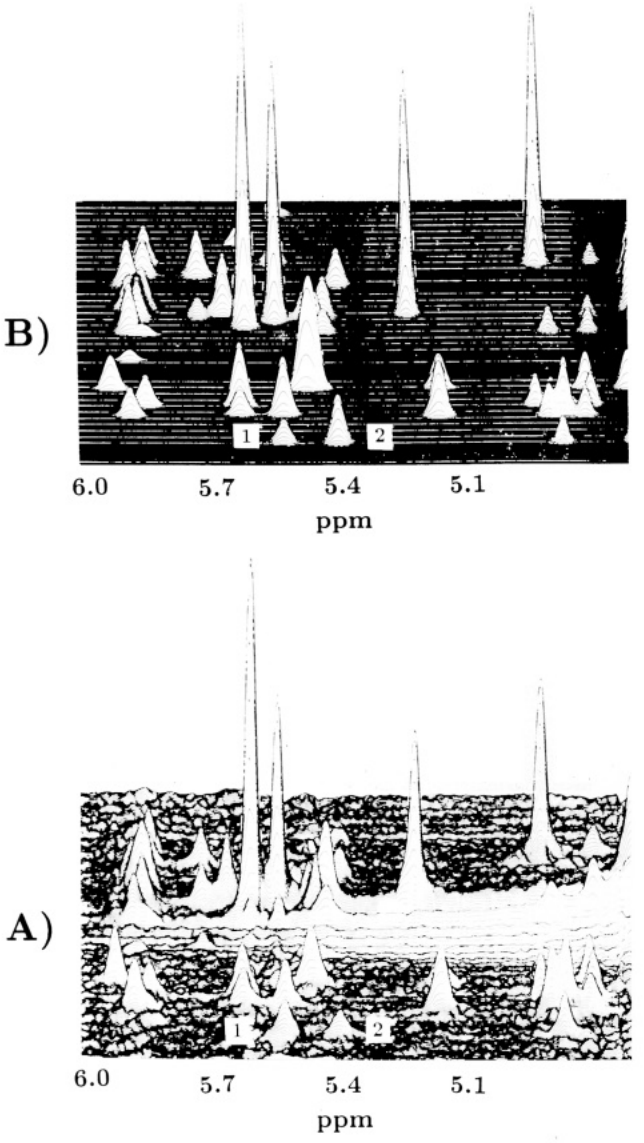

FIGURE 12: Stack plots of (A) the experimental and (B) the back-calculated 500-MHz ^{1}H NOESY spectrum of the H8/H6/H2 to 1′ region for [d(CGAGGTTTAAACCTCG)$_2$ in a canonical B-form DNA conformation.

chemical shift extrema of the unusually deshielded A9-H8 and the unusually shielded A9-H2 proton resonances in [d(CGAGGTTTAAACCTCG)]$_2$ and the corresponding A7-H8 and A7-H2 resonances in [d(GCCGTTAACGGC)]$_2$. Indeed, it is not surprising that the T8-N3H imino proton and A9-H2 both experience a shielding effect in the same direction since they are close in space and would be expected to reside in a common $P_2\cos(\theta)$ cone of the relevant ring-current field; i.e., the sign of the effect should be the same, while the more remote A9-H8 proton would be expected to reside outside the ring-current field cone with an opposite sign for the shift and thus be deshielded rather than shielded. This is also borne out by the T_2A_2 and T_3A_3 dodecamer structures reported by Kim and Reid (1992).

Complete NMR determination of the solution structure of hexadecamers will prove to be more formidable than for dodecamers. This is due not only to the spectral complexity but also to the effects of increasingly anisotropic rotational diffusion as the length to diameter ratio of the DNA helix increases (Duben & Hutton, 1990; Withka et al., 1990, 1991; Wang et al., 1992a). For 2D-NOESY data of equal quality with respect to both signal-to-noise ratio and resolution, data

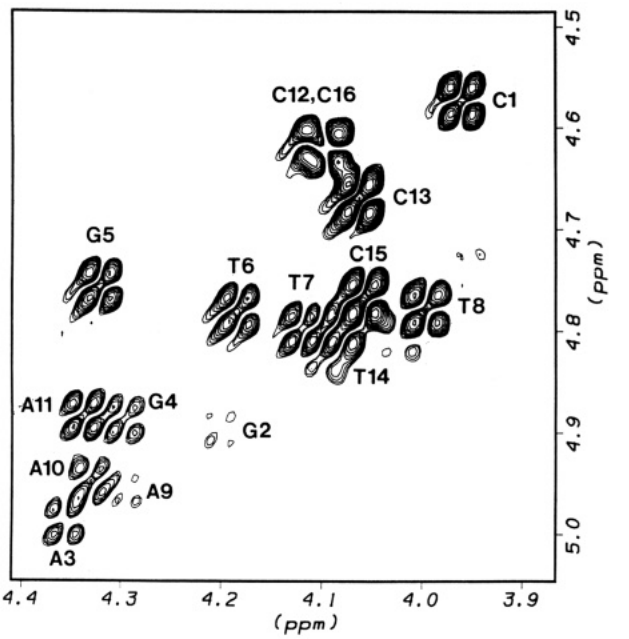

FIGURE 13: H3′–H4′ region of the 500-MHz ^{1}H DQF-COSY spectrum of [d(CGAGGTTTAAACCTCG)]$_2$ at 31 °C.

interpretation is intrinsically more difficult for longer duplexes because NOE crosspeak intensities in simulations can be matched to the experimental intensities by adjusting either the interproton distance or the polar angle that the interproton vector subtends with the helix axis. Hence, equal quality data sets will lead to an inherently less precise structure for hexadecamers. While a complete distance geometry structure for [d(CGAGGTTTAAACCTCG)]$_2$ is not immediately forthcoming due to a combination of the problems outlined above, J coupling has not been shown to be affected by anisotropic diffusion, and the following interesting structural features should be mentioned.

In the ECOSY spectrum of [d(CGAGGTTTAAACCTCG)]$_2$, the H2″–H3′ couplings are unobservable for all residues and the H1′–H2′ couplings are strong (data not shown), as expected for B-DNA (Kim et al., 1992). However, from an analysis of the H3′ to H4′ crosspeaks in the 500-MHz ^{1}H DQF-COSY spectrum shown in Figure 13, only two of the furanose sugar rings assume a C2′-endo conformation, i.e., exhibit very weak $J_{3'4'}$ couplings[1] indicating $P \approx 160$. These two sugars correspond to the first purine of the two purine runs in [d(CGAGGTTTAAACCTCG)]$_2$, namely, G2 in the GAGG tract and A9 in the AAA tract. In the AAA fragment, A10 has an intermediate crosspeak intensity and the intensity of A11 is strong (indicating a lower P value); in the GAGG fragment, A3 and G4 have intermediate crosspeak intensities, while the intensity of G5 is strong. These data indicate that the sugar conformation undergoes a progressive

[1] The possibility that the weak crosspeaks were due to partial cancellation of unusually broadened H3′ and/or H4′ resonances was examined. On the basis of the A9-H8 to A9-H3′ NOESY crosspeak, the A9-H3′ line width is not unusual. Similarly, from an anlaysis of the A9-H1′ to A9-H4′ NOESY crosspeak, the A9-H4′ resonance is not unusually broadened. The A9-H1′ to A9-H4′ 150-ms NOESY crosspeak is, however, about 2 times weaker than each of the other resolved H1′ to H4′ crosspeaks. This is consistent with a higher pseudorotation angle for the A9 sugar, i.e., a longer H1′-H4′ and a weaker H3′-H4′ crosspeak. The G2-H3′ and G2-H4′ resonances both have typical line widths based on the H1′ to H3′ and H1′ to H4′ NOESY crosspeaks. Interestingly, however, the H1′ to H4′ 150-ms NOESY crosspeak is similar to that of the other low P sugar residues. This may be due to distance averaging in this penultimate residue.

transition to lower pseudorotation phase angles in the 5′ to 3′ direction in both the AAA and GAGG tracts, i.e., from 2′-endo ($P \approx 162°$) at G2 and A9 to around 1′-exo ($P \approx 126°$) at G5 and A11, respectively. All other H3′-H4′ DQF-COSY crosspeak intensities are readily detectable, indicating that the remaining sugars all assume a conformation that is closer to the C1′-exo conformation than to the C2′-endo conformation. The gradual 2′-endo to 1′-exo transition in purine tracts may or may not be related to the reduced minor groove width at the outside edges of the T_3A_3 tract [strong (n)H2 to (m + 1)H1′ NOEs] and the unusual structure at the TpA central junction. It is worth noting that while the $J_{3'-4'}$ couplings tend to increase along the T_3 tract in the 5′ to 3′ direction, being strongest (lowest P value) at T8, there is a striking difference in sugar conformation between T8 (high J, low P) and A9 (low J, high P) at the TpA step, which is most certainly diagnostic of the unusual structure of the TpA junction. The dramatic difference in sugar conformation at the TpA junction is most likely the *result* of poor base stacking at the TpA step (Ornstein et al., 1978) rather than the *cause* of the distortion.

DISCUSSION

The H8 and H2 protons of the adenine base, which reside in the major and minor grooves, respectively, have both been shown to be motionally broadened at the TpA junction in T_nA_n tracts (where $n \geq 2$). This observation serves to confirm the general presence of conformational dynamics in T_3A_3 sequences as well as in the T_2A_2 sequences studied by Jardetzky and co-workers (Lefevre et al., 1985, 1988) and by Lane (1989, 1991). At the same time, the TpA H8 and H2 resonances are notably deshielded and shielded, respectively, due to an unusual average conformation of the adenine base at the junction. The excellent spectral resolution in the sequences chosen for study now allows us to address the question of whether the observed mobility is spread throughout the TTTAAA segment or is localized to a single site in this segment. The simples model, which we favor and which explains all of the experimental observations, is one in which only the TpA junction adenine is conformationally mobile. Hence, the protons of the neighboring "static" adenine bases are considered to be broadened by the reciprocal fluctuating ring-current field of the mobile adenine. An alternative model, which has been promoted by Lefevre et al. (1985, 1988), is that the neighboring bases are also mobile.

Our observations indicate that, while the H2 and H8 protons of the first adenine both experience internal motion that is on the fast side of coalescence, these two lines are also *both noticeably broadened* by conformational exchange on the chemical shift time scale. Interestingly, in the studies on the trp promoter TTAA sequence, excessive H8 broadening of the TpA adenine was reported in one case [see Table II in Lefevre et al. (1987)], but in a subsequent study on the same sequence, a thermodynamic analysis of the conformational transitions was justified on the basis that no differential line broadening of the TpA adenine H8 was observed (Lefevre et al., 1988). If excessive H8 broadening of the TpA adenine was in fact present but could not be measured due to poor resolution [the TpA adenine H8 resonance was only shown as part of the complete one-dimensional proton spectrum in Figure 1 of Lefevre et al. (1987)], then the strict assumption by Lefevre et al. (1988) of rapid exchange for the thermodynamic analysis of the temperature-dependent chemical shift of the TpA adenine H8 proton is weakened. In the studies of the mutant trp operator by Lane (1989, 1991), the TpA adenine H8 *does* show excessive line broadening.

Line-shaping simulations shown here demonstrate that the unusual broadening of these H2 and H8 resonances can be explained by chemical exchange (motion) at rates inferred from the experimental data. For aromatic H2 protons, whose chemical shifts can be modulated by neighboring ring-current shift effects as large as 1.4–1.6 ppm. i.e., 700–800 Hz at 500-MHz ^{1}H frequency, the observed 10-Hz broadening corresponds to a relatively slow purine motion, specifically at a rate on the order of 6–100 kHz. The rate of this motion is about 2 orders of magnitude faster than the proposed rate of exchange (200–250 s^{-1}) between the three structural states of the trp promoter TTAA sequence invoked by Lefevre et al. (1988). The 200–250-s^{-1} rate of exchange reported by Lefevre et al. (1988) appears to be inconsistent with the temperature-dependent $T_{1\rho}$ data in our present study. The discrepancy may be explained by two possibilities. First, the model put forward by Lefevre et al. (1988), i.e., transitions among three conformational states, may be too simple. Admittedly, they state that the three-state model is the simplest model that satisfied their data and that other multistate models may work equally well. Consider, for example, the case for which the state/transitions are better described by a diffusive process. The number of conformational states will increase and the enthalpy difference between states will decrease, thus leading to an increase in the transition rate between conformational states and better agreement with the $T_{1\rho}$ data collected in our present study. Second, the discrepancy may indicate that, while localized mobility at the TpA junction is a general phenomenon in T_nA_n sequences, the specific rate is context dependent. The motion examined in this study can be nicely explained by an oscillation about the adenosine glycosidic bond with an amplitude of 20–50 °C; the glycosidic torsion angle at the TpA step in the TTAA Pribnow box was reported to vary by only 10° between states states I and III in the study by Lefevre et al. (1988) but by as much as 30° in the mutant promoter TTAA sequence studied by Lane (1991). Other sharp contrasts exist in the structural features of the T_nA_n segment described by Lefevre et al. (1988) compared to this work. For example, Lefevre et al. (1988) claim that the first T in the trp promoter TTAA segment assumes a North conformation with $P = 20°$, while we clearly find the sugar conformation of the analogous penultimate T in the TTTAAA segment to be closer to the South conformation with $P \approx 126°$. They find that there is no difference between the P value of the sugars involved in the TpA or ApA steps in TTAA, whereas we find a striking pattern of changes in the sugar conformations in the TTTAAA segment, i.e., T_8 (126°), A_9 (162°), A_{10} (144°), A_{11} (126°), and in fact, in extensive studies on a variety of T_2A_2 and T_3A_3 dodecamers and hexadecamers in this laboratory (Kim & Reid, 1992; Kim and Reid, unpublished results), we find no T residues (or any other residues) in the N form.

In any case, the time scale of the motion is certainly too slow to modulate the NOE cross-relaxation rate via double-quantum transition probabilities. The zero-quantum spectral density, which dominates the NOESY cross-relaxation rate for correlation times in the spin–diffusion limit, should still be dominated by the effective global correlation time (≈5 ns rad^{-1}) for tumbling of the 16 base-pair DNA duplex, i.e., $1/\tau_c^{tot} = 1/\tau_c^{fast} + 1/\tau_c^{slow} \approx 1/\tau_c^{fast}$. However, if the amplitude were sufficiently large, and if the motion caused a significant variation of the interproton distances, then the simultaneous emphasis on all closest-approach pairwise distances could create problems in determining the actual structure at the TpA junction. In B-form DNA the (n)H8

and (*n*)H2 to (*n*)H1′ distance varies by only 0.2 Å for the proposed magnitude of oscillation about the glycosidic torsion angle and would not introduce any serious distance errors. On the other hand, the (*n*)A-H8 to (*n*)H2′ distance varies by ≈1 Å for a variation in χ form from −70° to −160°, i.e., a 90° oscillation. Our results indicate that the amplitude of motion/oscillation is at most ±25°, which would lead to a range of H8–H2′ interproton distances of up to 0.5 Å in a worst case scenario. Therefore, in a distance geometry structure refinement, the maximum effect of the motion on distance measurement could be accommodated by estimating the distance from the two-spin approximation and then simply widening the bounds to ±0.25 Å (or by using the estimate as a lower bound and setting the upper bound to be 0.5 Å longer than the two-spin approximated distance if it is assumed to be a heavily r^{-6}-weighted closest-approach estimate); this range is only slightly larger than the bounds range of ±0.15 Å normally used for H8 to H2′ distances. Lane (1990) has incorporated the effects of slow conformational averaging in structure refinement by taking population-weighted means of the conformations present. The rotating-frame relaxation data alone give no direct information on the amplitude of the motion. Because both the chemical shift dispersion and the rate of the motion can be independently varied to match the experimental line width, the full amplitude of the motion can only be limited to 20–50° from the present experiments. The amplitude of this mobility should, however, be quite amenable to study by solid-state NMR studies of duplexes containing deoxyadenosine labeled with deuterium in the C2 position; such studies are currently being pursued.

The physical origin of such a relatively slow motion at the center of T_nA_n tracts might be related to the observed widening of the minor groove at the TpA junction and to the unusual conformation of the adenine at the junction, which probably results from poor base stacking between the thymine and the adenine. The combination of these two structural features may allow the adenine at the TpA junction to have an unusual degree of motional freedom. This motional freedom may reflect local mobility in an otherwise rigid DNA helix (i.e., oscillation about the glycosidic bond), or it may reflect flexibility of the entire DNA helix at the TpA junction—possibly a time-dependent twist, tilt, or propeller-twist between two rigid segments of B′-DNA (Lefevre et al., 1988). It may be important to consider and/or incorporate either local mobility or TpA junction flexibility into theories of DNA bending or curvature to account for the quite different migration patterns of A_nT_n and T_nA_n DNA sequences in gel electrophoresis.

Finally, it is most interesting that the family of restriction enzymes that specifically recognize T_nA_n fragments of DNA, e.g., *Aha*III, *Pme*I, and *Hpa*I, all cleave the phosphodiester bond in the backbone precisely at the TpA junction. Mobility, coupled to distinct structural features such as base stacking or sugar conformations characteristic of the TpA junction, appears to play an intriguing role in protein–DNA recognition and in accessing the conformation required for hydrolysis of this phosphodiester bond.

ACKNOWLEDGMENT

We thank N. Susan Ribeiro and Julie Miller for synthesizing the DNA oligomers. We gratefully acknowledge Mary Coventry for help in preparing the manuscript and Andy Wang for helpful discussions.

REFERENCES

Abragam, A. (1961) in *Principles of Nuclear Magnetism* (Adair, R. K., Elliott, R. J., Marshall, W. C., & Wilkinson, D. H., Eds.) pp 309–312 Clarendon Press, Oxford, U.K.
Ailion, D., & Slichter, C. P. (1964) *Phys. Rev. Lett. 12*, 168–171.
Alam, T. M., & Drobny, G. (1990) *Biochemistry 29*, 3421–3430.
Allison, S. A., & Schurr, J. M. (1979) *Chem. Phys. 41*, 35–39.
Bax, A., & Davis, D. G. (1985) *J. Magn. Reson. 63*, 207–213.
Brash, D. E., & Haseltine, W. A. (1982) *Nature 298*, 189–192.
Burkhoff, A. M., & Tullius, T. D. (1988) *Nature 331*, 455–457.
Calladine, C. R., Drew, H. R., & McCall, M. J. (1988) *J. Mol. Biol. 201*, 127–137.
Celda, B., Widmer, H., Leupin, W., Chazin, W. J., Denny, W. A., & Wüthrich, K. (1989) *Biochemistry 28*, 1462–1471.
Chuprina, V. P. (1987) *Nucleic Acids Res. 15*, 293–311.
Chuprina, V. P., & Abagyan, R. A. (1988) *J. Biomol. Struct. Dyn. 6*, 121–138.
Chuprina, V. P., Federoff, O. Y., & Reid, B. R. (1991a) *Biochemistry 30*, 561–568.
Chuprina, V. P., Lipanov, A. A., Federoff, O. Y., Kim, S.-G., Kintanar, A., & Reid, B. R. (1991b) *Proc. Natl. Acad. Sci. U.S.A. 88*, 9087–9091.
Deverell, C., Morgan, R. E., & Strange, J. H. (1970) *Mol. Phys. 18*, 553–559.
Diekmann, S. (1987) *Nucleic Acids Res. 15*, 247–265.
Diekmann, S., & McLaughlin, L. W. (1988) *J. Mol. Biol. 202*, 823–834.
Diekmann, S., & Wang, J. C. (1985) *J. Mol. Biol. 186*, 1–11.
Diekmann, S., von Kitzing, E., McLaughlin, L., Ott, J., & Eckstein, F. (1987) *Proc. Natl. Acad. Sci. U.S.A. 84*, 8257–8261.
Drobny, G. P., Pines, A., Sinton, S., Weitekamp, D. P., & Wemmer, D. E. (1979) *Faraday Symp. Chem. Soc. 13*, 49–55.
Duben, A. J., & Hutton, W. C. (1990) *J. Am. Chem. Soc. 112*, 5917–5924.
Eisinger, J., Shulman, R. G., & Szymanski, B. M. (1962) *J. Chem. Phys. 36*, 1721–1729.
Giessner-Prettre, C., & Pullman, B. (1970) *J. Theor. Biol. 27*, 87–95.
Giessner-Prettre, C., Pullman, B., Borer, P. N., Kan, L.-S., & Ts'o, P. O. P. (1976) *Biopolymers 15*, 2277–2286.
Gupta, G., Sarma, M. H., & Sarma, R. H. (1988) *Biochemistry 27*, 7909–7919.
Hagerman, P. J. (1986) *Nature 321*, 449–450.
Hagerman, P. J. (1988) in *Unusual DNA Structures* (Wells, R. D., & Harvey, S. C., Eds.) pp 225–236, Springer-Verlag, New York.
Hagerman, P. J. (1990) *Annu. Rev. Biochem. 59*, 755–781.
Haran, T. E., & Crothers, D. M. (1989) *Biochemistry 28*, 2763–2767.
Hare, D. R., & Reid, B. R. (1986) *Biochemistry 25*, 5341–5350.
Harris, R. K. (1983) in *Nuclear Magnetic Resonance Spectroscopy*, pp 91–92, 123–124, Pitman Publishing, Marshfield, MA.
Johnson, C. E., Jr., & Bovey, F. A. (1958) *J. Chem. Phys. 29*, 1012–1014.
Katahira, M., Sugeta, H., Kyogoku, Y., Fujii, S., Fujisawa, R., & Tomita, K.-I. (1988) *Nucleic Acids Res. 16*, 8619–8632.
Katahira, M., Sugeta, H., Kyogoku, Y., & Fujii, S. (1990a) *Biochemistry 29*, 7214–7222.
Katahira, M., Sugeta, H., & Kyogoku, Y. (1990b) *Nucleic Acids Res. 18*, 613–618.
Kearns, D. R. (1984) *CRC Crit. Rev. Biochem. 15*, 237–290.
Kim, S.-G., & Reid, B. R. (1992) *Biochemistry 31*, 12103–12116.
Kim, S.-G., Lin, L.-J., & Reid, B. R. (1992) *Biochemistry 31*, 3564–3574.
Kintanar, A., Klevit, R. E., & Reid, B. R. (1987) *Nucleic Acids Res. 15*, 5848–5862.

Kintanar, A., Huang, W.-C., Schindele, D. C., Wemmer, D. E., & Drobny, G. (1989) *Biochemistry 28*, 282–293.
Koo, H.-S., & Crothers, D. M. (1988) *Proc. Natl. Acad. Sci. U.S.A. 85*, 1763–1767.
Koo, H.-S., Wu, H.-M., & Crothers, D. M. (1986) *Nature 320*, 501–506.
Kopple, K. D., Wang, Y.-S., Cheng, A. G., & Bhandary, K. K. (1988) *J. Am. Chem. Soc. 110*, 4168–4176.
Kroon, P. A., Kreishman, G. P., Nelson, J. H., & Chan, S. I. (1974) *Biopolymers 13*, 2571–2592.
Lane, A. N. (1989) *Biochem. J. 259*, 715–724.
Lane, A. N. (1990) *Biochim. Biophys. Acta 1049*, 189–204.
Lane, A. N. (1991) *Biochem. J. 273*, 383–391.
Lefevre, J.-F., Lane, A., & Jardetzky, O. (1985) *FEBS Lett. 190*, 37–40.
Lefevre, J.-F., Lane, A. N., & Jardetzky, O. (1987) *Biochemistry 26*, 5076–5090.
Lefevre, J.-F., Lane, A. N., & Jardetzky, O. (1988) *Biochemistry 27*, 1086–1094.
Leroy, J.-L., Charretier, E., Kochoyan, M., & Gueron, M. (1988) *Biochemistry 27*, 8894–8898.
Levitt, M. H., & Freeman, R. (1981) *J. Magn. Reson. 43*, 65–80.
Luo, J., Sarma, M. H., Gupta, G., & Sarma, R. H. (1991) *Int. J. Quantum Chem. 18*, 213–229.
Marini, J. C., Weisberg, R., & Landy, A. (1977) *Virology 83*, 254–270.
Marion, D., & Wüthrich, K. (1983) *Bull. Biol. Res. Counc. 113*, 967–994.
Olson, W. K., Sarma, M. H., Sarma, R. H., & Sundaralingam, M. (1988) in *Structure & Expression. Volume 3: DNA Bending & Curvature*, Adenine Press, Schenectady, NY.
Ornstein, R. L., Rein, R., Breen, D. L., & Macelroy, R. D. (1978) *Biopolymers 17*, 2341–2360.
Rance, M., Sorensen, O. W., Bodenhausen, G., Wagner, G., Ernst, E. E., & Wüthrich, K. (1983) *Biochem. Biophys. Res. Commun. 117*, 479–485.
Robinson, B. H., Forgacs, G., Dalton, L. R., & Frisch, H. L. (1980) *J. Chem. Phys. 73*, 4688–4692.
Sandström, J. (1982) in *Dynamic NMR Spectroscopy*, pp 14–18, Academic Press, New York.
Sarma, M. H., Gupta, G., & Sarma, R. H. (1988) *Biochemistry 27*, 3423–3432.
Schmidt, P. G., & Edelheit, E. B. (1981) *Biochemistry 20*, 79–86.
Schmitz, U., Sethson, I., Egan, W. M., & James, T. L. (1992) *J. Mol. Biol. 227*, 510–531.
Selsing, E., Wells, R. D., Alden, C. J., & Arnott, S. (1979) *J. Biol. Chem. 254*, 5417–5422.
Shulman, R. G., Hilbers, C. W., Kearns, D. R., Reid, B. R., & Wong, Y. P. (1973) *J. Mol. Biol. 78*, 57–69.
States, D. J., Haberkorn, R. A., & Ruben, D. J. (1982) *J. Magn. Reson. 48*, 286–292.
Stellwagen, A., & Stellwagen, N. C. (1990) *Biopolymers 30*, 309–324.
Strange, J. H., & Morgan, R. E. (1970) *J. Phys. C 3*, 1999–2011.
Trifonov, E. N., & Sussman, J. L. (1980) *Proc. Natl. Acad. Sci. U.S.A. 77*, 3816–3820.
Trifonov, E. N., & Ulanovsky, L. E. (1988) in *Unusual DNA Structures* (Wells, R. D., & Harvey, S. C., Eds.) pp 173–188, Springer-Verlag, New York.
Ulanovsky, L. E., & Trifonov, E. N. (1987) *Nature 326*, 720–722.
Wang, A. C., Kim, S.-G., Flynn, P. F., Sletten, E., & Reid, B. R. (1992a) *J. Magn. Reson. 100*, 358–366.
Wang, A. C., Kennedy, M. A., Reid, B. R., & Drobny, G. (1992b) *J. Am. Chem. Soc. 114*, 6583–6585.
Wang, Y.-S., & Ikuta, S. (1989) *J. Am. Chem. Soc. 111*, 1243–1248.
Waugh, J. S., & Fessenden, R. W. (1957) *J. Chem. Phys. 79*, 846–849.
Wemmer, D. E., Chou, S. H., Hare, D. R., & Reid, B. R. (1985) *Nucleic Acids Res. 13*, 3755–3772.
Withka, J. M., Swaminathan, S., & Bolton, P. H. (1990) *J. Magn. Reson.* 386–390.
Withka, J. M., Swaminathan, S., Beveridge, D. L., & Bolton, P. H. (1991) *J. Am. Chem. Soc. 113*, 5041–5049.
Wu, H.-M., & Crothers, D. M. (1984) *Nature 308*, 509–513.